Ramia DEEB

ANALYSIS OF MAGNETIC FIELD IN PM SERVOMOTOR

ABSTRACT *The paper presents design of the PM servomotor M 718, which is designed of a solid rotor with permanent magnets mounted at its surface. The applied permanent magnet material belongs to the rare earth class NdFeB. 2D model of servomotor is created using AutoCAD program and the materials added to the model are chosen from FEMM library. A comparison of magnetic flux density for both no load and nominal load is presented. The paper focuses on the effect of operation temperature on the permanent magnets properties. Changes in the magnetic flux density inside the motor according to the rotor position angle are presented using Lua Script (programming language of FEMM).*

Keywords: *magnetic field, permanent magnet, servomotor, design, megnetic flux density, load, operation temperature, rotor position angle*

1. INTRODUCTION

Permanent magnet motors (PM motors) are preferred to be used because of their excellent properties. The PM synchronous motors in comparison with their induction counterparts do not have rotor winding losses that cause increas in their efficiency. The larger air gap in synchronous motors make them more reliable in comparison with induction motors. The power density of permanent

Ramia DEEB, Ph.D.
e-mail: xdeebr00@stud.feec.vutbr.cz

Brno University of Technology

PROCEEDINGS OF ELECTROTECHNICAL INSTITUTE, Issue 258, 2012

magnet synchronous motors is higher than the one of induction motors with the same ratings due to the no stator power dedicated to the magnetic field production. The PM synchronous motors are usually built with one of the following rotor configurations: interior-magnet rotor, surface-magnet rotor, inset--magnet rotor, rotor with buried magnets symmetrically distributed, rotor with buried magnets asymmetrically distributed. Applying of permanent magnet materials (PMs) in the electrical machines improves their efficiency by eliminating excitation losses. The air gap magnetic flux density increases, which means greater output power for the same main dimensions. The PM machines have been used only into a limited number of low power applications due to the relatively high price of the magnetic materials. However, in the last decade, the performance improvements and smaller costs of the magnets have made possible the utilization of that machine topology in a wide range of applications such as robotics, power tools and public life, etc. [1, 4].

2. THEORY OF PM SYNCHRONOUS MOTORS

Rotors in PM synchronous motors rotate synchronously with the rotating magnetic field produced by a poly-phase electric supply. The rotor speed n_s is given by the ratio of input frequency f to number of pole-pairs p [1],

$$n_s = f / p \tag{2.1.}$$

Because of the stator slots, the magnetic flux density in the air gap is non--sinusoidal. The first harmonic of the flux density in the air gap B_{mg1} is given as:

$$B_{mg1} = \frac{2}{\pi} \int_{-0.5\alpha_i\pi}^{0.5\alpha_i\pi} B_{mg} \cos\alpha \, d\alpha = \frac{4}{\pi} B_{mg} \sin\frac{\alpha_i \pi}{2} \tag{2.2.}$$

In the Eq. 2.2, the coefficient α_i is defined as the ratio of the average to maximum value of the air gap magnetic flux density:

$$\alpha_i = \frac{B_{avg}}{B_{mg}} = \frac{b_p}{\tau} \tag{2.3.}$$

where, b_p is pole shoe arc and τ is pole pitch.

Carter's coefficient k_c, magnetic flux density under the pole shoe B_{mg} that can be found according to the magnetomotive force MMF F_{exc} of excitation and the phase angle γ between the currents of the two layers are defined as:

$$k_c = \frac{t_1}{t_1 - \gamma_1 g} \tag{2.4}$$

$$B_{mg} = \mu_0 F_{exc} / (g' k_c) \tag{2.5}$$

$$\gamma_1 = \frac{4}{\pi}\left[\frac{b_{14}}{2g}\arctan\left(\frac{b_{14}}{2g}\right) - \ln\sqrt{1+\left(\frac{b_{14}}{2g}\right)^2}\right] \tag{2.6}$$

$$t_1 = \frac{\pi D_{in}}{s_1} \tag{2.7}$$

where, t_1 [mm] is slot pitch, g' equivalent air gap which includes PM height h_M and Carter's coefficient k_c, h_M [mm] is height of PM, b_{14} [mm] width of the stator slot opening, g [mm] is air gap, μ_0 [H/m] is magnetic constant (vacuum permeability), D_{in} [mm] is the inner diameter of stator, and s_1 number of stator slots.

Carter's coefficient k_c which can be calculated according to motor data, is given as follows:

b_{14} = 2 [mm], g = 0.7 [mm], D_{in} =63 [mm], s_1 = 18.

The paper presents the magnetic analysis of PM servomotor M 718. The magnetic analysis of this servomotor is computed according to the following scheme:

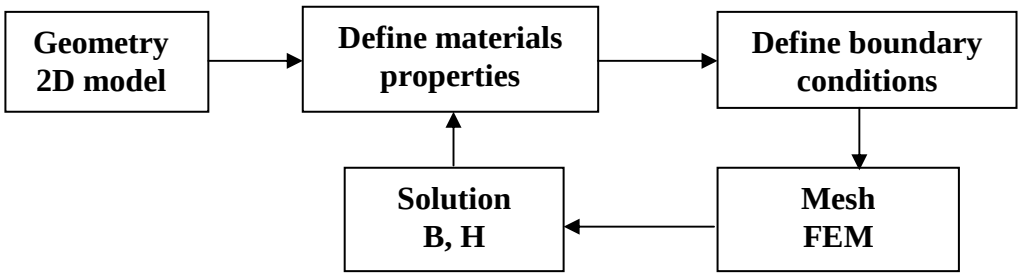

Fig. 1. Scheme of magnetic analysis

The first step of this analysis is to create a 2D model of the servomotor, then to define properties of material to the model of servomotor. The next step is to define the boundary conditions for this analysis, then generating the mesh and finally to solve the problem.

3. PHYSICAL MODEL OF THE SERVOMOTOR

The servomotor M 718 is produced by the VUES Brno s.r.o. company. The permanent magnet material applied to this servomotor is of rare earth NdFeB type. 2D model of the servomotor is created using the AutoCAD program and it is presented in Figure 2. The technical data of PM servomotor M 718 are as follows in Table 1.

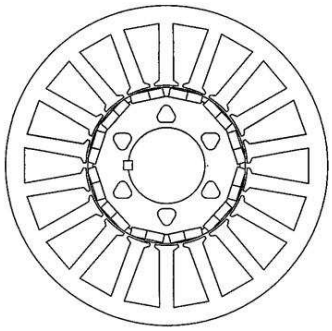

Fig. 2. 2D model of the servomotor M 718

TABLE 1
Parameters of the servomotor M 718I

Property	Value	Unit
Voltage	280	V
Current	11.56	A
Torque	16.5	Nm
Rotational speed	3000	rpm
Output power	5174	W
Number of pole pairs	6	–

4. MATERIAL PROPERTIES

The stainless steel material is used for both stator and rotor. The steel material is used for the shaft. The copper material is used for coils. NdFeB material is used for the permanent magnets, considering the correct direction of the magnetization in the permanent magnets (Polarization). Air is used to surround the servomotor model and for the air gap between rotor and stator in addition to the channels inside the rotor. Materials were chosen from the standard FEMM (finite element method magnetic) library, and according to datasheet of servomotor M 718 for permanent magnet material [6, 7].

5. BOUNDARY CONDITIONS

The first boundary condition is defined by considering the magnetic line $A_z = 0$ on an air area surrounding the motor. The second boundary condition is defined by setting the current density in the stator coils in the case of nominal load [3].

6. MAGNETIC ANALYSIS

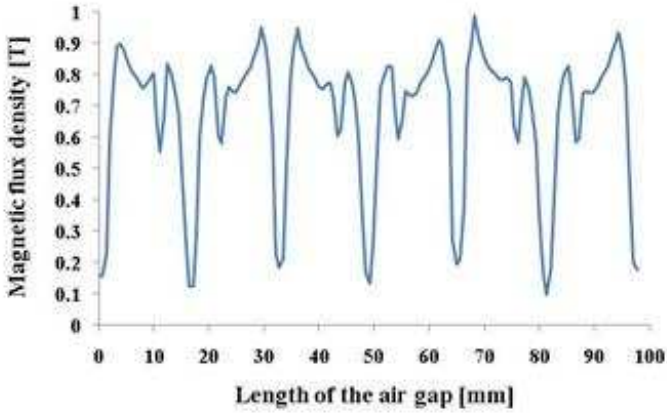

Fig. 3. Magnetic flux density in the air gap for no load

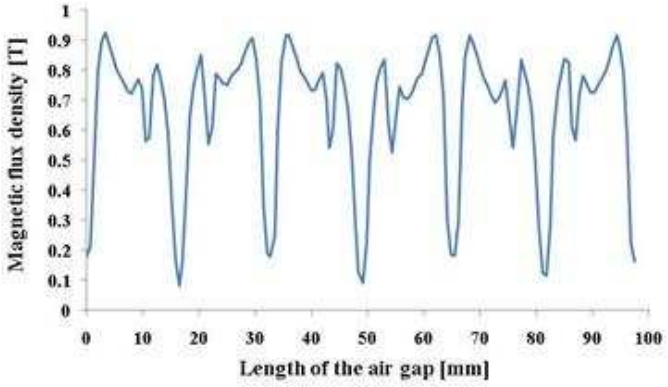

Fig. 4. Magnetic flux density in the air gap for nominal load

The magnetic analysis of servomotor M 718 has been computed for both no load and nominal load as follows in Figures 3 and 4; Figures present circumferential distribution of magnetic flux density in the air gap center for both no load and nominal load. The maximum and average values of magnetic flux density are computed and both are given in [T].

Two magnetic fields in PM motors exist, the magnetic field produced by the winding and the magnetic field produced by the permanent magnet on the rotor. The magnetic analysis of the servomotor is computed using the FEMM program.

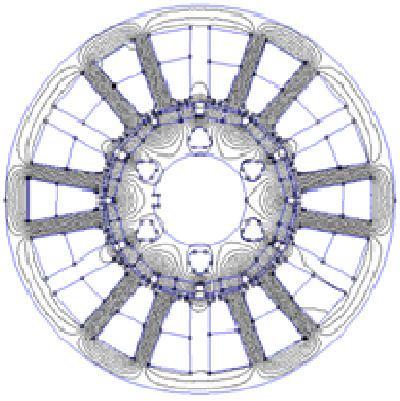

Fig. 5. Distribution of magnetic flux lines

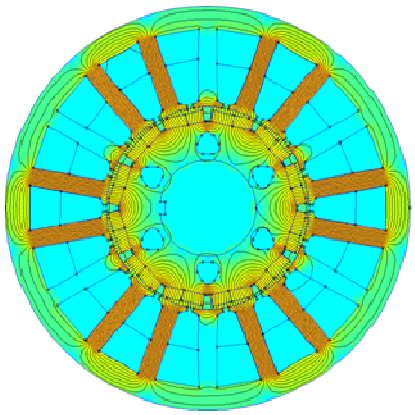

Fig. 6. Distribution of magnetic flux density

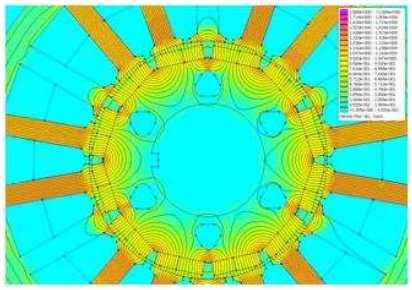

Fig. 7. Distribution of magnetic flux density in the rotor

The following figures present the distribution of the magnetic flux density in the different parts of the servomotor M 718. Figures 7 to 9 present distribution of the magnetic flux density in the rotor, in the permanent magnet and in the stator slot, respectively.

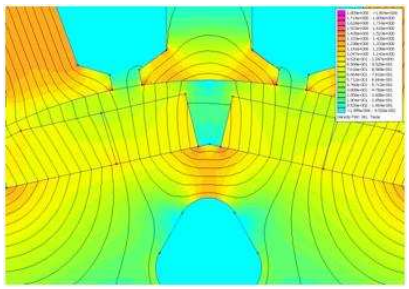

Fig. 8. Distribution of magnetic flux density in the permanent magnets

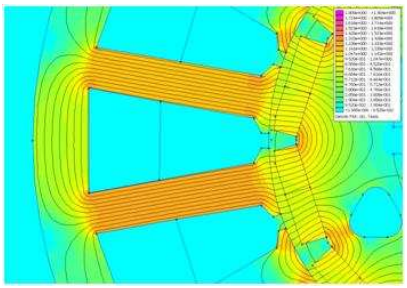

Fig. 9. Distribution of magnetic flux density in the stator slot

7. EFFECT OF TEMPERATURE ON PROPERTIES OF PERMANENT MAGNET MATERIAL

The permanent magnet materials may lose their magnetic properties if they are heated to a certain high temperature. Demagnetization curves of PMs are sensitive to the temperature, both remanent flux density B_r and coercivity H_c decrease with the increasing temperature of permanent magnets. Particularly for NdFeB material, which has relatively high temperature coefficients of remanent flux density and coercivity [1, 2].

$$B_r = B_{r20}\left[1+\frac{\alpha_B}{100}\left(\vartheta_{PM}-20\right)\right] \tag{7.1}$$

$$H_c = H_{c20}\left[1+\frac{\alpha_H}{100}\left(\vartheta_{PM}-20\right)\right] \tag{7.2}$$

where, B_{r20} remanent magnetic flux density at 20℃, [T], H_{c20} coercive force at 20℃, [kA/m], $\alpha_B < 0$ temperature coefficient for B_r, $\alpha_H < 0$ temperature coefficient for H_c, ϑ_{PM} permanent magnets temperature, [℃].

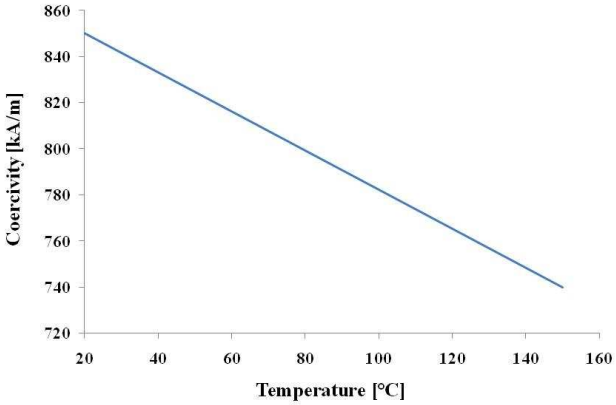

Fig. 10. Coercivity according to temperature for MagnetFabrik material

Figure 10 presents the changes in coercivity depending on operation temperature for the MagnetFabrik material $H_c = F(T)$, where, T is temperature, [℃] and H_c coercivity, [kA/m].

The effect of temperature on the magnetic flux density in the air gap is presented as follows:

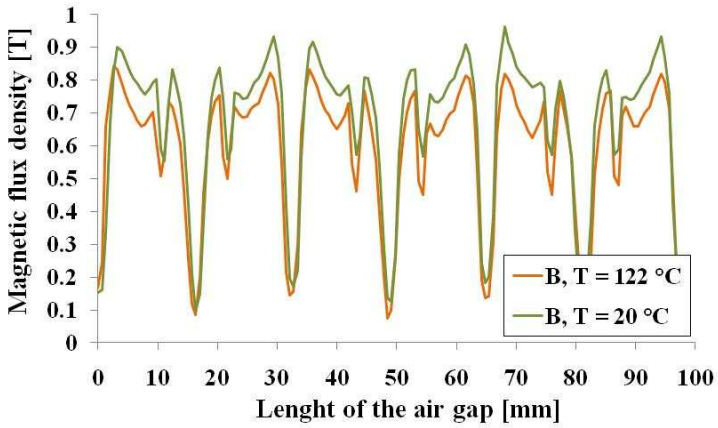

Fig. 11. Magnetic flux density at T = 20 ℃ and 122 ℃

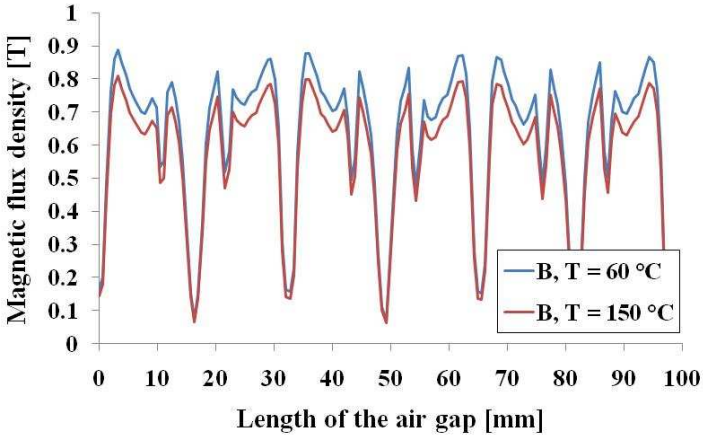

Fig. 12. Magnetic flux density at T = 60 ℃ and 150 ℃

Figures 11 to 12 present the magnetic flux density in the air gap at different temperatures considering that $T = 122$℃ is the steady state temperature of the servomotor M 718.

8. CHANGES IN THE MAGNETIC FIELD INSIDE THE SERVOMOTOR ACCORDING TO THE ROTOR POSITION ANGLE

Lua Script is used to show the changes in the magnetic field inside the servomotor. It is a programming language connected to the program FEMM. Thereby the rotor is controlled to rotate by a certain angle. The magnetic analysis at the steady state is presented in Figure 13.

Changes in the magnetic field during the servomotor operation as a function of the rotor position are presented in Figures 14 to 19.

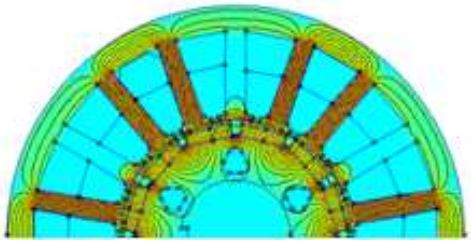

Fig. 13. Magnetic flux density at the steady state

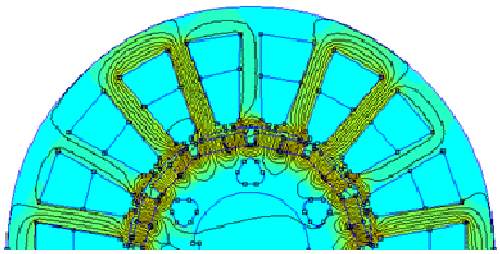

Fig. 14. Magnetic flux density at rotor position $\alpha = 0°$

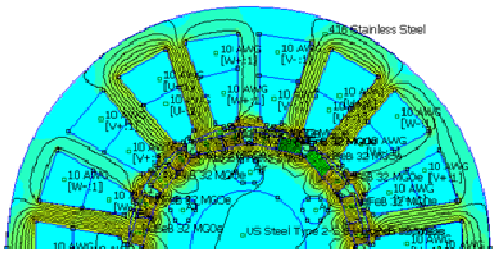

Fig. 15. Magnetic flux density at rotor position $\alpha = 60°$

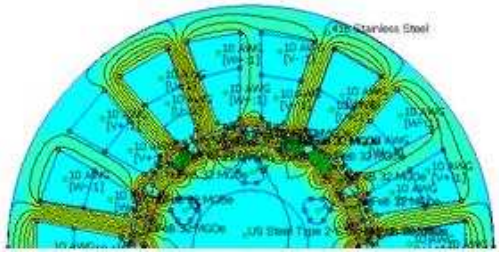

Fig. 16. Magnetic flux density at rotor position $\alpha = 120°$

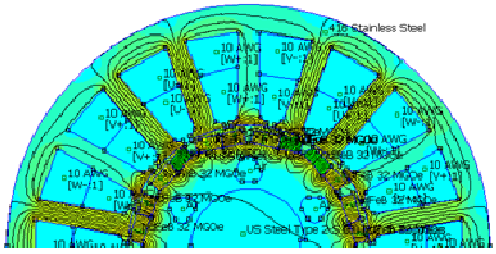

Fig. 17. Magnetic flux density at rotor position $\alpha = 180°$

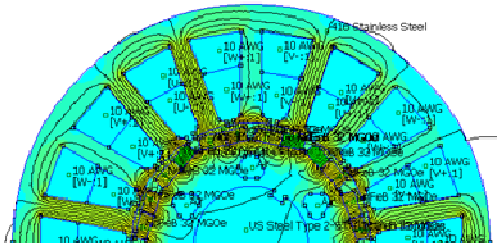

Fig. 18. Magnetic flux density at rotor position $\alpha = 240°$

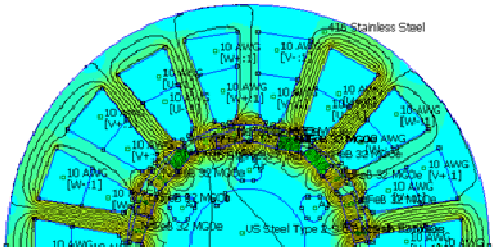

Fig. 19. Magnetic flux density at rotor position $\alpha = 300°$

9. CONCLUSION

The maximum magnetic flux density in the air gap for no load is of about 0.99 T (Fig. 3) and for nominal load it is 0.93 T (Fig. 4). The magnetic flux density decreases under load operation because of the armature reaction.

The magnetic behavior of PM servomotor M 718 has been presented in this paper. FEM analysis is used for this purpose.

Computed value of Carter's coefficient is about 1.3, while the calculated one is about 1.11. The difference between the two values is due to the approximation made in the value of the magnetic flux density in the air gap, in addition to the method error.

The other results presented in this paper concern the effect of operation temperature on the permanent magnet properties. The maximum value of the magnetic flux density in the air gap is 0.96 T at in temperature of 20℃, while the value decreases to about 0.80 T at the temperature of 150℃.

Acknowledgement

Author gratefully acknowledges financial support from European Regional Development Fund and from the Ministry of Education, Youth and Sports under projects CZ.1.05/2.1.00/01.0014 and FEKT S-11-9.

LITERATURE

1. Gieras J.F., Wing M.: Permanent Magnet Motor Technology, Design and applications Second, Edition, Revised and Expanded, New York, 2002.
2. Hwang C.C.; John S.B.; Bor S.S.: The analysis and design of a NdFeB permanent magnet spindle motor for CD-ROM drive, IEEE Transactions on Energy Conversion, Dec 1999, vol. 14, no. 4.
3. Wang X., Chen J., Wang P.: The magnetic field analysis of permanent magnet synchronous motor used in pure electric vehicle based on FEM, 2010 International Conference on Electrical Machines and Systems (ICEMS), Tianjin, China, Oct. 2010.
4. Almandoz G., Poza J., Rodriguez M. A., Gonzalez A.: Co-Simulation Tools for the Permanent Magnet Machine Design Oriented to the Application, The International Conference on Computer as a Tool, EUROCON 2007, Warsaw, Sept. 2007.
5. Hongfeng L., Changliang X., Peng S., Tingna S.: Magnetic Field Analysis of A Halbach Array PM Spherical Motor, 2007 IEEE International Conference on Automation and Logistics, Jinan, China, Aug. 2007.
6. Manual for program FEMM 4.2.
7. Servomotor M 718 technical datasheet (VUES company documentation).

Manuscript submitted 16.02.2012

ANALIZA POLA MAGNETYCZNEGO W SERWOMOTORZE Z MAGNESAMI TRWAŁYMI

Ramia DEEB

STRESZCZENIE *Artykuł przedstawia budowę serwomotoru z magnesami trwałymi M 718, który składa się z litego wirnika z magnesami trwałymi umieszczonymi na jego powierzchni. Zastosowane magnesy twałe należą NdFeB ziem rzadkich. Dwuwymiarowy model serwomotoru stworzono przy użyciu programu AutoCAD, stosując materiały z biblioteki FEMM. Porównano gęstośc strumienia magnetycznego dla stanu bez obciążenia znamionowego. Artykuł skupia się na wpływie temperatury pracy na własności magnesów trwałych. Przedstawiono zmiany gęstości strumienia magnetycznego w silniku w zależności od kąta położenia wirnika, stosując Lua Script (język programowania FEMM).*

Słowa kluczowe: *pole magnetyczne, magnes trwały, serwomotor, budowa, gęstość strumienia magnetycznego, obciążenie, temperatura pracy, kąt położenia wirnika*